NASA Technical Memorandum 87706

Feasibility of a Nuclear Gauge for Fuel Quantity Measurement Aboard Aircraft

(NASA-TM-87706) FEASIBILITY OF A NUCLEAR GAUGE FOR FUEL QUANTITY MEASUREMENT ABOARD AIRCRAFT (NASA) 25 p HC A02/MF A01 CSCL 14B N86-28385
Unclas
G3/35 43370

Jag J. Singh, Gerald H. Mall,
Danny R. Sprinkle, and Hoshang Chegini

AUGUST 1986

NASA

NASA Technical Memorandum 87706

Feasibility of a Nuclear Gauge for Fuel Quantity Measurement Aboard Aircraft

Jag J. Singh
Langley Research Center
Hampton, Virginia

Danny R. Sprinkle
Langley Research Center
Hampton, Virginia

Gerald H. Mall
Computer Sciences Corporation
Hampton, Virginia

Hoshang Chegini
Old Dominion University
Norfolk, Virginia

NASA
National Aeronautics
and Space Administration

Scientific and Technical
Information Branch

1986

Summary

Capacitance fuel gauges have served as the basis for fuel quantity indicating systems in aircraft for several decades. However, there have been persistent reports by the airlines that these gauges often give faulty indications due to microbial growth and other contaminants in the fuel tanks. This report describes the results of a feasibility study of using gamma ray attenuation as the basis for measuring fuel quantity in the tanks. Studies with a weak Am^{241} 59.5-keV radiation source indicate that it is possible to continuously monitor the fuel quantity in the tanks to an accuracy of better than 1 percent. These measurements also indicate that there are easily measurable differences in the physical properties and resultant attenuation characteristics of JP-4, JP-5, and Jet A fuels. The experimental results, along with a suggested source-detector geometrical configuration, are described.

Introduction

Capacitance fuel gauges have served as the basis for fuel quantity indicating systems in aircraft for several decades. These gauges, in the form of concentric cylinders, are mounted vertically at several locations inside the fuel tanks (ref. 1). The summations of their indications give the total tank fuel content at any time. However, there have been persistent reports (ref. 2) by the airlines that the capacitance gauges often give faulty indications of tank fuel contents. The problem has been attributed to microbial growth and/or contaminants in the fuel tanks. The microbes can occur in storage tanks, delivery lines, pump trucks, and consequently, in the aircraft fuel tanks. The microbes attack the capacitance cylinder coatings and thus expose the cylinder surfaces (electrodes) for subsequent corrosion and electrical noise in the capacitance bridge circuit. They also corrode the output signal leads. It is thus highly desirable that a fuel quantity indicating system insensitive to fuel contamination be developed. Such a system should be highly accurate (better than 1 percent), safe to use and operate, and inexpensive.

An investigation of the feasibility of using gamma ray attenuation as the basis for measuring the fuel quantity in aircraft tanks has been conducted. The results of these studies are described in the following sections.

Principle of Operation of a Nuclear Gauge

The operation of a nuclear gauge is based on the attenuation of gamma rays passing through matter. As a result of interaction of gamma rays with the atoms in the test medium, the number of unaffected primary photons arriving at the detector is a function of the path length in the test medium. For a uniform medium, it is given by the following expression (ref. 3):

$$I_x = I_o e^{-\mu x} \tag{1}$$

where

I_x	number of unaffected primary photons transmitted through test medium
I_o	number of photons incident on test medium
μ	linear attenuation coefficient for incident photons in test medium
x	path length in test medium

Clearly, such a gauge will be more sensitive if the attenuation coefficient (μ) is large for the incident photons. This dictates the choice of low-energy (less than 100 keV) photon sources. Two plausible candidate sources that meet the necessary criteria of low photon energy, long source half-life, and a well-resolved photon spectrum are Am^{241} (458 years) and Cd^{109} (453 days).

The decay schemes (ref. 4) for these two sources are shown in figures 1 and 2, respectively. It is noted that the 59.5-keV radiation from the Am^{241} source results from a super-allowed electric dipole (E1) transition in Np^{237}, whereas the 87.7-keV radiation from the Cd^{109} source arises from a weakly allowed electric octopole (E3) transition in Ag^{109}. The latter transition is strongly internally converted and produces a large, lower energy Ag K X-ray flux. For example, a 10-mCi Am^{241} disc source emits 7.4×10^6 photons (59.5 keV) per second per steradian, whereas a 10-mCi Cd^{109} source emits 2.6×10^7 photons (22.6 keV) per second per steradian (ref. 5). The relative intensities of gamma rays and characteristic X-Rays emitted from these sources are summarized in table I (ref. 4). Thus, even though the choice of a Cd^{109} source will necessitate changing the source every 3 years or so, Cd^{109} still appears to be a viable candidate source by virtue of its large lower energy photon yield.

Experimental Procedures for Measuring Attenuation Coefficients

Since the *exact* compositions of aviation fuels are seldom known (refs. 6 and 7), it was not possible to calculate their attenuation coefficients for Am^{241} and Cd^{109} gamma rays. It was therefore decided to determine the attenuation coefficients of selected types of fuels experimentally.

Attenuation coefficients of several samples of commercial aviation fuels were measured in the narrow beam geometry illustrated in figure 3. The fuel cells were made of glass and were fabricated in the form of 3-in. (7.62-cm) diameter flat-ended cylinders of three different lengths for easy data reduction. The gamma rays were detected with a 2-in. (5.08-cm) diameter × 2-in. (5.08-cm) thick NaI (Tl) crystal coupled to a high-gain photomultiplier. Figure 4 shows the geometrical details of the source, collimators, fuel cells, and detector assembly.

Measurements were made with empty fuel cells and cells filled with the test fluids. To further test the sensitivity of the system, measurements were also made with distilled water in the fuel cells. Typical Am^{241} and Cd^{109} spectra are shown in figures 5 and 6.

For the Am^{241} source, the single-channel analyzer (SCA) limits were adjusted to accept the strong 59.5-keV peak. For the Cd^{109} source, the SCA limits were set to accept the weaker 87.7-keV total capture peak rather than the stronger, but unresolved, lower energy Ag K_α (22.1 keV) and Ag K_β (25.0 keV) peaks.

The nominal radioactive source strengths readily available for this test were of the order of 10 μCi (Am^{241}) and 100 μCi (Cd^{109}). They provided good counting statistics for all test fluids over a period of 10 minutes. Measurements were made *with* and *without* the source in each case to subtract the counts due to cosmic rays and other background sources of radiation.

The attenuation coefficients were measured for water, JP-4 fuel, JP-5 fuel, Jet A fuel, regular leaded automobile gasoline, and unleaded automobile gasoline.

Data Reduction and Results

Counts were recorded for 10 minutes for each source for the three fuel cells filled with the test fluids. The geometrical details of the configurations incorporating test cells G-2, G-3, and G-4 are shown in figure 4. Typical results are summarized in table II.

As illustrated in figure 4, the photons have to pass through air, glass fuel cell ends, test fluid, and a 0.079-cm-thick aluminum housing for the NaI (Tl) crystal before arriving at the detector surface, that is,

$$I_x = I_o \left(e^{-\mu_{air} x_{air}} e^{-\mu_{glass} x_{glass}} \times e^{-\mu_{fluid} x_{fluid}} e^{-\mu_{Al} x_{Al}} \right) \qquad (2)$$

The values of μ_{air} and μ_{Al} at 59.5 keV and 87.7 keV have been reported by a number of authors (refs. 8 to 10). With these values, I_o can be easily calculated from equation (2) if the entire path length is made up of air and aluminum. If an empty glass fuel cell is introduced in the path of the beam, the drop in the counting rate provides a direct measure of μ_{glass} for the incident photons. If the fuel cells are filled with the test fluids, the changes in the counting rates will reflect the effects of attenuation characteristics of the test fluids. The experimental values of linear attenuation coefficients of the various test fluids are summarized in table III. These values are based on several independent sets of data of the type summarized in table II.

Since the mass attenuation coefficients[1] of the media are of more fundamental value than the linear attenuation coefficients (ref. 3), it was necessary to determine the densities of the test fluids. The densities of all the fluids were measured with a standard 50-ml pycnometer, and these values were used to calculate the mass attenuation coefficients of the test fluids. These results are also included in table III. It is interesting to note that there are easily measurable differences in the attenuation coefficients of various test fluids.

Subsequent to the measurements of the respective attenuation coefficients of all the test fluids for the Am^{241} and Cd^{109} gamma rays, it was finally decided to test the sensitivity of attenuation of low-energy photons as the basis for a fuel gauging system aboard aircraft. The wing tank geometry for a Boeing 737 airplane was selected for the computer model as representative of all aircraft with positive wing tip inclination with respect to the horizontal while on the ground. The computational procedures and the program developed for calculations for an Am^{241} gamma ray source and Jet A fuel test medium are described below.

Computational Procedure

The computer program WNGTNK is written in FORTRAN Version 5 language for the Control Data CYBER 170 series digital computer system with network operating system (NOS) 2.3. The program requires approximately 40 000 octal locations of core storage. A typical case requires less than 4 central processing unit (CPU) seconds on the CYBER 173.

The wing tank (Boeing 737) modeled by the program is illustrated in figure 7. For purposes of modeling, each of the 14 compartments in this figure is approximated by a rectangular box. Any similar wing

[1] The mass attenuation coefficients are independent of the actual density and physical state (gas, liquid, or solid) of the absorber.

tank can be modeled by this technique by simply adjusting the number of compartments and the dimensions of each rectangular box. Figure 8 illustrates the tank model as viewed from the front of the aircraft with the fuselage (not shown) to the left. The program provides the user with the capability of specifying the height of the bottom of each compartment, B_i, to simulate the bending of the wing associated with flight conditions. The solid dot $(\cdot)$ in each compartment depicts the source location, SL, and the detectors are assumed to be fixed to the bottom of each compartment. Table IV summarizes the specific data used in the modeling of the Boeing 737, where W_i, H_i, and D_i are the compartment widths, heights, and depths, respectively.

Once the tank geometry has been defined, the program steps through fixed percentages of tank fuel capacity. For each amount of fuel, the fuel level is computed with the assumption of a level fuel surface. With the fuel level known, the path length between each source–detector pair occupied by fuel or air is determined. From these path lengths, the number of counts is determined. The baffles between compartments contained in the wing structure are assumed to absorb radiation, so there is no interference between adjacent compartments.

Program input consists of 14 numbers, separated by commas, representing the height, B_i, of each compartment bottom in inches. Program output includes both tabular and graphic results.

Typical results corresponding to the configuration of figure 8 are included as table V and are illustrated in figure 9. These data were acquired with a source strength of about 30 μCi at each station in a counting interval of 1 second. Obviously, this system has a fast response time (approximately 1 second) and high resolution (approximately 1 percent). In this figure, each line depicts the relationship between counts and fuel expended for a specific compartment, with the lines toward the right nearer the wing tip and the lines toward the left nearer the fuselage. In particular, note that when the tank is full, the counting rates are the same in each compartment, since the path lengths through fuel are all equal. As fuel is expended, the counting rates change first in those compartments near the wing tip. After approximately 35 percent of the fuel has been expended, the compartment nearest the tip is empty and shows no further change in counting rate. Also note that the source in compartment 1 is completely immersed in the fuel until approximately 85 percent of the fuel is expended and begins to show a change in counting rate as the fuel is reduced below this level. Figure 9 also shows that significant changes in counts can be observed in one or more compartments as the fuel level varies, regardless of the tank contents.

A listing of the computer program used in this analysis is included as an appendix.

Discussion

For the sake of specificity, we will confine our discussions to the results for an Am^{241} (59.5-keV) gamma source. Similar results are expected for a Cd^{109} (87.7-keV) gamma source.

As seen from the data in table V, the counting rate is constant at all stations when the tank is full. A 1-percent reduction in the fuel content in the tank causes a large increase (about 56.9 percent) in the counting rate at the wing tip detector (station 14). A further reduction of 1 percent in the fuel causes an additional increase (about 26.6 percent) in the counting rate at the wing tip detector. It also results in a counting rate increase of about 16.2 percent at station 13. These counting rate changes are easily measurable. The same trend continues as more fuel is consumed. For example, when 10 percent of the fuel has been consumed, the total cumulative counting rate increases at stations 14, 13, and 12 are 238.6, 114.6, and 35.9 percent, respectively. At the other end of the spectrum when the tank is nearly empty, the counting rates in the outer station detectors have stabilized, but the counting rates at the stations near the fuselage are changing fast. For example, when the tank is only 5 percent full, the counting rates at stations 1, 2, and 3 are 330.1, 521.0, and 822.6 percent higher than the counting rate for the full tank. A further reduction of 1 percent in the fuel causes the counting rates to increase to 392.3, 619.1, and 977.1 percent of the values for the full tank, respectively.

From these data it is apparent that the fuel quantity gauging system detailed in this report is capable of detecting changes as low as 1 percent in the fuel contents at the two extreme limits, that is, when the tank is almost full and when it is almost empty. A careful examination of table V illustrates that a similar degree of sensitivisty exists for all levels of tank fuel contents.

From the foregoing discussion, it is apparent that a continuous monitoring of counting rates at all the detector stations should enable continuous tracking of airplane fuel tank contents with a high degree of sensitivity.

Concluding Remarks

It has been demonstrated that a suitably designed nuclear gauge should enable a continuous monitoring of the tank fuel contents to an accuracy of better than 1 percent. Such accurate information—both at the point of flight origination when the tanks are presumably full and at the final destination when the tanks are almost empty—should prove very useful to the airlines. It should provide reliable information about the payload capacity at the beginning of the flight and safety margin near the end of the flight. The nuclear gauge is not expected to be susceptible to the fouling and corrosion problems experienced by the conventional capacitance gauges, since both the source and the radiation detector are sealed. Any algae or microbial growth on the source and detector windows can be easily removed during scheduled periodic maintenance checks of the gauging system.

An added advantage of the nuclear gauge is its inherent capability to detect water buildup in the tank. Since water is expected to gravitate toward the fuselage, any reduction in the counting rates at stations 1 through 5 when the tank is at least half full can be used to infer the quantity of water in the tank. It is also a self-calibrating system with a high degree of cross-checking capability. This capability renders the nuclear gauging system independent of any background count rate changes with altitude. (In any case, changes in background count rate at altitudes less than 10 miles are expected to be minimal in the SCA window centered at 59.5 keV.)

It should perhaps be noted that despite the large low-energy photon flux obtainable with a Cd^{109} source, an Am^{241} source would be more economical, since it would require no source replacement because of its long half-life. It would also be comparatively safer to handle and/or shield because of its lower energy. As a matter of fact, Am^{241}-based densitometers are currently in use aboard some aircraft. The licensing requirements for an Am^{241}-based fuel quantity measurement system would be no different from what they are for those aircraft. By an appropriate choice of the Am^{241} source strength, the response time of the nuclear gauge can be safely arranged to be less than 1 second.

The effects of temperature on the fuel volume can be easily taken care of by simultaneous—but independent—measurements of temperature and density. These measurements will also enable real-time computation of fuel mass (as opposed to fuel volume) at any time in flight or on the ground.

NASA Langley Research Center
Hampton, VA 23665-5225
May 6, 1986

References

1. Newport, Ronald L.; Nelson, Donald J.; and Manfred, Mark T.: Digital Fuel Quantity Indicating System for Aircraft. *Proceedings of the AIAA/IEEE 6th Digital Avionics Systems Conference*, Dec. 1984, pp. 21–27. (Available as AIAA-84-2602.)
2. *Wing Tank Microbial Growth and Corrosion—Boeing/Airline Regional Conference.* Boeing Commercial Airplane Co., 1980.
3. Evans, Robley D.: *The Atomic Nucleus.* McGraw-Hill Book Co., Inc., c.1955.
4. Lederer, C. Michael; Hollander, Jack M.; and Perlman, Isadore: *Table of Isotopes,* Sixth ed. John Wiley & Sons, Inc., c.1967.
5. *Du Pont NEN Products U.S. Price List.* E. I. du Pont de Nemours & Co. (Inc.), Mar. 1, 1985.
6. Barnett, Henry C.; and Hibbard, Robert R.: *Properties of Aircraft Fuels.* NACA TN 3276, 1956. (Supersedes NACA RM E53A21 and NACA RM E53116.)
7. Coordinating Res. Council, Inc.: *Handbook of Aviation Fuel Properties.* CRC Rep. No. 530, 1983. (Available from DTIC as AD A132 106.)
8. Grodstein, Gladys White: *X-Ray Attenuation Coefficients From 10 kev to 100 Mev.* NBS Circ. 583, U.S. Dep. Commerce, Apr. 30, 1957.
9. McGinnies, Rosemary T.: *X-Ray Attenuation Coefficients From 10 kev to 100 Mev.* Suppl. to NBS Circ. 583, U.S. Dep. Commerce, Oct. 30, 1959.
10. Davisson, Charlotte Meaker; and Evans, Robley D.: Gamma-Ray Absorption Coefficients. *Rev. Mod. Phys.*, vol. 24, no. 2, Apr. 1952, pp. 79–107.

TABLE I. RELATIVE INTENSITIES OF CHARACTERISTIC X-RAYS AND GAMMA RAYS EMITTED FROM Am^{241} AND Cd^{109} RADIOACTIVE SOURCES

Am^{241} source		Cd^{109} source	
Photon energy (keV)	Relative intensity	Photon energy (keV)	Relative intensity
11.89 (Np L_l)	2.2	22.1 (Ag K_α)	25.5
13.90 (Np L_α)	37.5	25.0 (Ag K_β)	5.0
17.80 (Np L_β)	51.2		
20.80 (Np L_γ)	13.8	87.7	1.0
26.35	7.0		
59.50	100.0		

TABLE II. COUNTS PER 10-MINUTE INTERVAL FOR VARIOUS TEST MEDIA WITH Am^{241} AND Cd^{109} SOURCES[a]

Test medium	Am^{241} source			Cd^{109} source		
	Cell G-2 $L_2 = 4.982$ cm	Cell G-3 $L_2 = 7.522$ cm	Cell G-4 $L_2 = 10.062$ cm	Cell G-2 $L_2 = 4.982$ cm	Cell G-3 $L_2 = 7.522$ cm	Cell G-4 $L_2 = 10.062$ cm
Air (no cell)	75446	49988	35710	43650	30476	23184
Air (empty cell)	54489	36705	25491	35404	24897	18906
JP-4 fuel	27880	13899	7480	21080	12950	9192
JP-5 fuel	26859	13204	7018	20765	12569	9018
Jet A fuel	26816	12918	7229	20322	12431	8802
Leaded gasoline	28732	14462	7981	21110	13105	9233
Unleaded gasoline	28966	14353	8094	20948	13107	9202
Water	22095	9832	5267	18455	10937	8001
Background	1817	1850	1876	5319	5391	5270

[a]See figure 4 for geometrical details of fuel cell and associated shields/collimators.

TABLE III. SUMMARY OF ATTENUATION COEFFICIENTS FOR VARIOUS TEST FLUIDS

Test fluid	Test fluid density, ρ, g/cm^3	Am^{241} (59.5 keV) source		Cd^{109} (87.7 keV) source	
		μ, cm^{-1}	μ_m cm^2/g	μ, cm^{-1}	μ_m, cm^2/g
JP-4 fuel	0.7546	0.143 ± 0.003	0.190 ± 0.004	0.127 ± 0.002	0.169 ± 0.003
JP-5 fuel	0.8097	0.150 ± 0.002	0.185 ± 0.003	0.134 ± 0.004	0.165 ± 0.005
Jet A fuel	0.8107	0.150 ± 0.002	0.185 ± 0.003	0.137 ± 0.002	0.168 ± 0.003
Leaded gasoline	0.7300	0.135 ± 0.001	0.185 ± 0.002	0.126 ± 0.003	0.172 ± 0.004
Unleaded gasoline	0.7443	0.135 ± 0.002	0.182 ± 0.003	0.125 ± 0.002	0.167 ± 0.003
Water	0.9974	0.194 ± 0.002	0.194 ± 0.002	0.165 ± 0.002	0.166 ± 0.002

TABLE IV. DATA USED FOR BOEING 737 WING TANK MODEL

[Source type—Am^{241} (59.5 keV); source strength—10^6 counts per second; source enclosure—0.01-in.-thick aluminum]

Compartment	W, in.	H, in.	D, in.	B, in.	SL, in.
1	24.0	26.8	82.0	0.0	8.2
2	24.0	24.6	78.0	1.5	8.2
3	24.0	22.6	73.0	3.0	8.2
4	24.0	20.6	68.0	4.5	8.2
5	24.0	18.6	63.0	6.0	8.2
6	24.0	16.6	58.0	7.5	8.2
7	24.0	14.6	53.0	9.0	8.2
8	24.0	13.6	49.8	10.5	8.2
9	24.0	12.7	46.5	12.0	8.2
10	24.0	11.8	43.2	13.5	8.2
11	24.0	10.9	39.9	15.0	8.2
12	24.0	10.0	36.6	16.5	8.2
13	24.0	9.1	33.3	18.0	8.2
14	24.0	8.2	30.0	19.5	8.2

TABLE V. SUMMARY OF THE COUNTING RATES AT VARIOUS STATIONS AS A FUNCTION OF THE FUEL IN THE WING TANK

Fuel content, percent	Counts per second in compartment— 1	2	3	4	5	6	7	8	9	10	11	12	13	14
.00	4558	4558	4558	4558	4558	4558	4558	4558	4558	4558	4558	4558	4558	4558
1.00	2839	4481	4558	4558	4558	4558	4558	4558	4558	4558	4558	4558	4558	4558
2.00	2209	3486	4558	4558	4558	4558	4558	4558	4558	4558	4558	4558	4558	4558
3.00	1753	2766	4366	4558	4558	4558	4558	4558	4558	4558	4558	4558	4558	4558
4.00	1475	2328	3674	4558	4558	4558	4558	4558	4558	4558	4558	4558	4558	4558
5.00	1241	1959	3093	4558	4558	4558	4558	4558	4558	4558	4558	4558	4558	4558
6.00	1070	1688	2665	4206	4558	4558	4558	4558	4558	4558	4558	4558	4558	4558
7.00	936	1477	2332	3680	4558	4558	4558	4558	4558	4558	4558	4558	4558	4558
8.00	819	1293	2041	3221	4558	4558	4558	4558	4558	4558	4558	4558	4558	4558
9.00	720	1136	1793	2830	4467	4558	4558	4558	4558	4558	4558	4558	4558	4558
10.00	644	1017	1606	2535	4000	4558	4558	4558	4558	4558	4558	4558	4558	4558
11.00	577	911	1438	2270	3582	4558	4558	4558	4558	4558	4558	4558	4558	4558
12.00	517	816	1288	2033	3208	4558	4558	4558	4558	4558	4558	4558	4558	4558
13.00	463	731	1154	1822	2875	4537	4558	4558	4558	4558	4558	4558	4558	4558
14.00	421	665	1049	1656	2614	4126	4558	4558	4558	4558	4558	4558	4558	4558
15.00	383	604	954	1506	2377	3751	4558	4558	4558	4558	4558	4558	4558	4558
16.00	376	549	867	1369	2161	3410	4558	4558	4558	4558	4558	4558	4558	4558
17.00	376	499	789	1245	1965	3101	4558	4558	4558	4558	4558	4558	4558	4558
18.00	376	455	719	1135	1791	2827	4462	4558	4558	4558	4558	4558	4558	4558
19.00	376	418	660	1043	1646	2598	4100	4558	4558	4558	4558	4558	4558	4558

TABLE V. Continued

Fuel content, percent	Counts per second in compartment — 1	2	3	4	5	6	7	8	9	10	11	12	13	14
20.00	376	384	607	958	1512	2387	3767	4558	4558	4558	4558	4558	4558	4558
21.00	376	376	558	880	1390	2193	3462	4558	4558	4558	4558	4558	4558	4558
22.00	376	376	512	809	1277	2016	3181	4558	4558	4558	4558	4558	4558	4558
23.00	376	376	471	743	1173	1852	2923	4558	4558	4558	4558	4558	4558	4558
24.00	376	376	436	688	1086	1714	2705	4269	4558	4558	4558	4558	4558	4558
25.00	376	376	403	637	1006	1587	2505	3954	4558	4558	4558	4558	4558	4558
26.00	376	376	376	590	932	1470	2321	3663	4558	4558	4558	4558	4558	4558
27.00	376	376	376	547	863	1362	2150	3393	4558	4558	4558	4558	4558	4558
28.00	376	376	376	506	799	1262	1991	3143	4558	4558	4558	4558	4558	4558
29.00	376	376	376	469	740	1169	1845	2911	4558	4558	4558	4558	4558	4558
30.00	376	376	376	437	690	1089	1718	2712	4280	4558	4558	4558	4558	4558
31.00	376	376	376	407	643	1015	1602	2528	3990	4558	4558	4558	4558	4558
32.00	376	376	376	379	599	946	1493	2356	3719	4558	4558	4558	4558	4558
33.00	376	376	376	376	558	882	1392	2196	3467	4558	4558	4558	4558	4558
34.00	376	376	376	376	520	822	1297	2047	3231	4558	4558	4558	4558	4558
35.00	376	376	376	376	485	766	1209	1908	3012	4558	4558	4558	4558	4558
36.00	376	376	376	376	453	715	1129	1782	2813	4439	4558	4558	4558	4558
37.00	376	376	376	376	424	670	1058	1669	2635	4159	4558	4558	4558	4558
38.00	376	376	376	376	397	628	991	1564	2468	3895	4558	4558	4558	4558
39.00	376	376	376	376	376	588	928	1465	2312	3649	4558	4558	4558	4558
40.00	376	376	376	376	376	551	869	1372	2166	3418	4558	4558	4558	4558
41.00	376	376	376	376	376	516	814	1285	2029	3202	4558	4558	4558	4558

TABLE V. Continued

Fuel content, percent	Counts per second in compartment—													
	1	2	3	4	5	6	7	8	9	10	11	12	13	14
42.00	376	376	376	376	376	483	763	1204	1900	2999	4558	4558	4558	4558
43.00	376	376	376	376	376	453	716	1130	1783	2814	4442	4558	4558	4558
44.00	376	376	376	376	376	426	673	1062	1677	2647	4177	4558	4558	4558
45.00	376	376	376	376	376	401	633	999	1577	2489	3928	4558	4558	4558
46.00	376	376	376	376	376	377	595	940	1483	2341	3695	4558	4558	4558
47.00	376	376	376	376	376	376	560	884	1395	2202	3475	4558	4558	4558
48.00	376	376	376	376	376	376	526	831	1312	2070	3268	4558	4558	4558
49.00	376	376	376	376	376	376	495	782	1234	1947	3073	4558	4558	4558
50.00	376	376	376	376	376	376	466	735	1160	1831	2890	4558	4558	4558
51.00	376	376	376	376	376	376	439	693	1095	1728	2727	4304	4558	4558
52.00	376	376	376	376	376	376	414	654	1033	1630	2573	4061	4558	4558
53.00	376	376	376	376	376	376	391	617	974	1538	2428	3832	4558	4558
54.00	376	376	376	376	376	376	376	582	919	1451	2291	3615	4558	4558
55.00	376	376	376	376	376	376	376	549	867	1369	2161	3411	4558	4558
56.00	376	376	376	376	376	376	376	518	818	1292	2039	3218	4558	4558
57.00	376	376	376	376	376	376	376	489	772	1219	1924	3037	4558	4558
58.00	376	376	376	376	376	376	376	462	729	1150	1816	2866	4524	4558
59.00	376	376	376	376	376	376	376	437	689	1088	1718	2712	4280	4558
60.00	376	376	376	376	376	376	376	413	652	1030	1625	2565	4049	4558
61.00	376	376	376	376	376	376	376	391	617	974	1538	2427	3830	4558
62.00	376	376	376	376	376	376	376	376	584	922	1455	2296	3624	4558
63.00	376	376	376	376	376	376	376	376	552	872	1376	2172	3428	4558

TABLE V. Continued

Fuel content, percent	Counts per second in compartment—													
	1	2	3	4	5	6	7	8	9	10	11	12	13	14
64.00	376	376	376	376	376	376	376	376	522	825	1302	2055	3243	4558
65.00	376	376	376	376	376	376	376	376	494	780	1232	1944	3068	4558
66.00	376	376	376	376	376	376	376	376	468	738	1165	1839	2903	4558
67.00	376	376	376	376	376	376	376	376	443	700	1105	1743	2752	4343
68.00	376	376	376	376	376	376	376	376	420	663	1047	1653	2609	4118
69.00	376	376	376	376	376	376	376	376	398	629	993	1567	2474	3904
70.00	376	376	376	376	376	376	376	376	378	596	941	1486	2346	3702
71.00	376	376	376	376	376	376	376	376	376	565	893	1409	2224	3510
72.00	376	376	376	376	376	376	376	376	376	536	846	1336	2109	3328
73.00	376	376	376	376	376	376	376	376	376	508	802	1267	1999	3155
74.00	376	376	376	376	376	376	376	376	376	482	761	1201	1895	2992
75.00	376	376	376	376	376	376	376	376	376	457	721	1139	1797	2837
76.00	376	376	376	376	376	376	376	376	376	433	684	1080	1704	2689
77.00	376	376	376	376	376	376	376	376	376	411	648	1023	1616	2550
78.00	376	376	376	376	376	376	376	376	376	389	615	970	1532	2418
79.00	376	376	376	376	376	376	376	376	376	376	583	920	1452	2292
80.00	376	376	376	376	376	376	376	376	376	376	553	872	1377	2174
81.00	376	376	376	376	376	376	376	376	376	376	524	827	1306	2061
82.00	376	376	376	376	376	376	376	376	376	376	497	784	1238	1954
83.00	376	376	376	376	376	376	376	376	376	376	471	743	1174	1853
84.00	376	376	376	376	376	376	376	376	376	376	446	705	1113	1756
85.00	376	376	376	376	376	376	376	376	376	376	423	668	1055	1665

TABLE V. Concluded

Fuel content, percent	Counts per second in compartment—													
	1	2	3	4	5	6	7	8	9	10	11	12	13	14
86.00	376	376	376	376	376	376	376	376	376	376	401	634	1000	1579
87.00	376	376	376	376	376	376	376	376	376	376	380	601	948	1497
88.00	376	376	376	376	376	376	376	376	376	376	376	570	899	1419
89.00	376	376	376	376	376	376	376	376	376	376	376	540	853	1346
90.00	376	376	376	376	376	376	376	376	376	376	376	511	807	1273
91.00	376	376	376	376	376	376	376	376	376	376	376	483	762	1203
92.00	376	376	376	376	376	376	376	376	376	376	376	456	719	1136
93.00	376	376	376	376	376	376	376	376	376	376	376	427	674	1063
94.00	376	376	376	376	376	376	376	376	376	376	376	399	629	994
95.00	376	376	376	376	376	376	376	376	376	376	376	376	585	923
96.00	376	376	376	376	376	376	376	376	376	376	376	376	538	850
97.00	376	376	376	376	376	376	376	376	376	376	376	376	490	774
98.00	376	376	376	376	376	376	376	376	376	376	376	376	437	690
99.00	376	376	376	376	376	376	376	376	376	376	376	376	376	590
100.00	376	376	376	376	376	376	376	376	376	376	376	376	376	376

Appendix

Listing of Computer Programs

Program WNGTNK

```
      PROGRAM WNGTNK(OUTPUT,INPUT,TAPE6=OUTPUT,TAPE5=INPUT)
      COMMON/GEOMTY/W(14),H(14),D(14),B(14),SL(14),VTOT,NC
      COMMON/ANS/COUNTS(14,101)
      DIMENSION FRAC(101)
      INTEGER COUNTS
      DATA ERROR/1.E-5/
    1 FORMAT(1H1,45X,'SUMMARY OF COUNTS'////
     1 5X,'% LIQUID',45X,'COMPARTMENT'/
     2 18X,'   1   ','   2   ','   3   ','   4   ','   5   ',
     3 '   6   ','   7   ','   8   ','   9   ','  10   ',
     4 '  11   ','  12   ','  13   ','  14   '//)
    2 FORMAT(1H0,5X,F7.2,2X,14I7)
      CALL PSEUDO
      CALL CALPLT(1.,1.,-3)
      CALL INIT
      NCM = NC - 1
      NFILL = 101
      READ(5,*,END=10) B
   10 IF(EOF(5).NE.0) GO TO 120
      ISGN = -1
      V = -0.01*VTOT
      DO 100 K=1,NFILL
      ISGN = -ISGN
      DVOL = 0.01*VTOT
      V = V + DVOL
      FRAC(K) = 100.*V/VTOT
      Z = 0.
      DO 20 I=1,NCM
      Z = B(I+1)
      V1 = 0.
      DO 20 J=1,I
      TOP = Z
      BOTTOM = B(J)
      IF(TOP.GT.(B(J) + H(J))) TOP = B(J) + H(J)
      V1 = V1 + D(J)*W(J)*(TOP - BOTTOM)
      IF(V1.GT.V) GO TO 30
   20 CONTINUE
      I = NC
   30 CONTINUE
      J = I - 1
      VBOT = 0.
      IF(J.EQ.0) GO TO 50
      DO 40 I=1,J
      Z = B(J+1)
      TOP = Z
      BOTTOM = B(I)
      IF(TOP.GT.(B(I) + H(I))) TOP = B(I) + H(I)
      VBOT = VBOT + D(I)*W(I)*(TOP - BOTTOM)
   40 CONTINUE
   50 CONTINUE
      J = J + 1
      ZOLD = B(J)
      DZ = B(J) + 0.75*H(J)
   60 CONTINUE
      V1 = 0.
      ZMAX = 0.
      DO 70 I=1,J
      IF((B(I) + H(I)).GT.ZMAX) ZMAX = B(I) + H(I)
```

```
      TOP = ZOLD
      BOTTOM = B(J)
      IF(TOP.GT.(B(I) + H(I))) TOP = B(I) + H(I)
      IF(BOTTOM.GT.(B(I) + H(I))) BOTTOM = B(I) + H(I)
      V1 = V1 + D(I)*W(I)*(TOP - BOTTOM)
   70 CONTINUE
      VOLUME = VBOT + V1
      TSTV = V
      IF(V.EQ.0.) TSTV = 1.
      IF(ABS(VOLUME - V)/TSTV.LT.ERROR) GO TO 90
      IF(VOLUME.LT.V) GO TO 80
      ZOLD = ZOLD - DZ
      DZ = 0.5*DZ
      GO TO 60
   80 ZOLD = ZOLD + DZ
      GO TO 60
   90 CONTINUE
      IF(ZOLD.GT.ZMAX) ZOLD = ZMAX
      CALL TABL(ZOLD,K)
      IF(K.EQ.1) CALL PICT(ZOLD)
  100 CONTINUE
      WRITE(6,1)
      DO 110 I=1,NFILL
      WRITE(6,2) FRAC(I),(COUNTS(K,I),K=1,NC)
  110 CONTINUE
      CALL PLTCNT
  120 CONTINUE
      CALL CALPLT(0.,0.,999)
      STOP
      END
```

Subroutine INIT

```
      SUBROUTINE INIT
      COMMON/GEOMTY/W(14),H(14),D(14),B(14),SL(14),VTOT,NC
      NC = 14
      D(1) = 82.
      D(2) = 78.
      D(3) = 73.
      D(4) = 68.
      D(5) = 63.
      D(6) = 58.
      D(7) = 53.
      D(8) = 49.8
      D(9) = 46.5
      D(10) = 43.2
      D(11) = 39.9
      D(12) = 36.6
      D(13) = 33.3
      D(14) = 30.
      H(1) = 26.8
      H(2) = 24.6
      H(3) = 22.6
      H(4) = 20.6
      H(5) = 18.6
      H(6) = 16.6
      H(7) = 14.6
      H(8) = 13.6
      H(9) = 12.7
      H(10) = 11.8
      H(11) = 10.9
      H(12) = 10.
      H(13) = 9.1
      H(14) = 8.2
      VTOT = 0.
```

```
      DO 10 I=1,NC
      W(I) = 24.
      VTOT = VTOT + W(I)*H(I)*D(I)
   10 CONTINUE
      NCO2 = NC/2
      DO 20 I=1,NC
      SL(I) = 8.2
   20 CONTINUE
      RETURN
      END
```

Subroutine PICT

```
      SUBROUTINE PICT(Z)
      COMMON/GEOMTY/W(14),H(14),D(14),B(14),SL(14),VTOT,NC
      DIMENSION XA(35),YA(35),XB(35),YB(35)
      DATA EPS/1.E-4/
      IND = 1
      X = 0.
      Y = 0.
      XI = 0.
      YI = 1.0*(B(NC) + H(NC))/34.
      CALL CALPLT(XI,YI,3)
      XA(IND) = XI
      YA(IND) = YI
      IF(1.*Z/34..LT.YI) YA(IND) = 1.*Z/34.
      IF(YA(IND).LT.1.*B(NC)/34.) YA(IND) = 1.*B(NC)/34.
      IND = IND + 1
      DO 10 I=1,NC
      X = X + W(NC+1-I)/34.
      Y = 1.0*(B(NC+1-I) + H(NC+1-I))/34.
      CALL CALPLT(X,Y,2)
      XA(IND) = X - EPS
      YA(IND) = Y
      IF(1.*Z/34..LT.Y) YA(IND) = 1.*Z/34.
      IF(YA(IND).LT.1.*B(NC+1-I)/34.) YA(IND) = 1.*B(NC+1-I)/34.
      IND = IND + 1
      IF(I.NE.NC)
     1Y = 1.0*(B(NC-I) + H(NC-I))/34.
      IF(I.EQ.NC) Y = 0.
      CALL CALPLT(X,Y,2)
      XA(IND) = X + EPS
      YA(IND) = Y
      IF(1.*Z/34..LT.Y) YA(IND) = 1.*Z/34.
      IF(YA(IND).LT.1.*B(NC-I)/34.) YA(IND) = 1.*B(NC-I)/34.
      IND = IND + 1
   10 CONTINUE
      CALL CALPLT(XI,YI,3)
      X = XI
      Y = 1.0*B(NC)/34.
      CALL CALPLT(X,Y,2)
      IND = 1
      XB(IND) = X
      YB(IND) = Y
      IND = IND + 1
      DO 20 I=1,NC
      X = X + W(NC+1-I)/34.
      Y = 1.0*B(NC+1-I)/34.
      CALL CALPLT(X,Y,2)
      XB(IND) = X - EPS
      YB(IND) = Y
      IND = IND + 1
      IF(I.EQ.NC) GO TO 20
```

```
      Y = 1.0*B(NC-I)/34.
      CALL CALPLT(X,Y,2)
      XB(IND) = X + EPS
      YB(IND) = Y
      IND = IND + 1
   20 CONTINUE
      XA(29) = 0.
      XB(29) = 0.
      XA(30) = 1.
      XB(30) = 1.
      YA(29) = 0.
      YB(29) = 0.
      YA(30) = 1.
      YB(30) = 1.
      NP = 28
C     CALL HAFTONE(XA,YA,NP,XB,YB,NP,9)
      CALL LINPLT(XA,YA,NP,1,0,0,0,0)
      XI = -0.5*W(14)/34.
      DO 30 I=1,NC
      XI = XI + W(NC-I+1)/34.
      YI = 1.*(B(NC-I+1) + SL(NC-I+1))/34.
      CALL PNTPLT(XI,YI,22,1)
   30 CONTINUE
      CALL NFRAME
      CALL CALPLT(1.,1.,-3)
      RETURN
      END
```

Subroutine TABL

```
      SUBROUTINE TABL(Z,K)
      COMMON/GEOMTY/W(14),H(14),D(14),B(14),SL(14),VTOT,NC
      COMMON/ANS/COUNTS(14,101)
      REAL LIQSIG,LIQDEN
      INTEGER COUNTS
      DATA AIRSIG,AIRDEN,LIQSIG,LIQDEN,ALSIG,ALDEN/
     1 0.178,0.001293,0.150,.7999,0.248,2.7/
      DATA STRNGT/1.E+6/
      PI = ACOS(-1.)
      DO 10 I=1,NC
      HEIGHT = H(I)
      TOP = Z
      IF(TOP.GT.(H(I)+B(I))) TOP = H(I) + B(I)
      IF(TOP.LT.B(I)) TOP = B(I)
      SLDANG = 10.*2.54/(4.*PI*(2.54*SL(I))**2)
      DLIQ = TOP - B(I)
      DAIR = SL(I) - DLIQ
      IF(DLIQ.GT.SL(I)) DLIQ = SL(I)
      IF(DLIQ.EQ.SL(I)) DAIR = 0.
      XC = SLDANG*STRNGT
      XC = XC*EXP(-2.54*0.01*ALSIG*ALDEN)
      XC = XC*EXP(-2.54*DLIQ*LIQSIG*LIQDEN)
      XC = XC*EXP(-2.54*DAIR*AIRSIG*AIRDEN)
      COUNTS(I,K) = XC
   10 CONTINUE
      RETURN
      END
```

Subroutine PLTCNT

```
      SUBROUTINE PLTCNT
      COMMON/GEOMTY/W(14),H(14),D(14),B(14),SL(14),VTOT,NC
      COMMON/ANS/COUNTS(14,101)
      DIMENSION FRAC(101)
      INTEGER COUNTS
      DIMENSION X(105),Y(105)
      DO 30 J=1,NC
      X(102) = 0.
      X(103) = 10.
      Y(102) = 0.
      Y(103) = 600.
      IF(J.NE.1) GO TO 10
      CALL AXES(0.,0.,0.,10.,X(102),X(103),1.,0.,
     1 8H% LIQUID,0.2,-8)
      CALL AXES(0.,0.,90.,8.,Y(102),Y(103),1.,0.,
     1 6HCOUNTS,0.2,6)
   10 CONTINUE
      DO 20 I=1,101
      X(I) = FLOAT(I-1)
      Y(I) = COUNTS(J,I)
   20 CONTINUE
      CALL LINPLT(X,Y,101,1,0,0,0,0)
   30 CONTINUE
      RETURN
      END
```

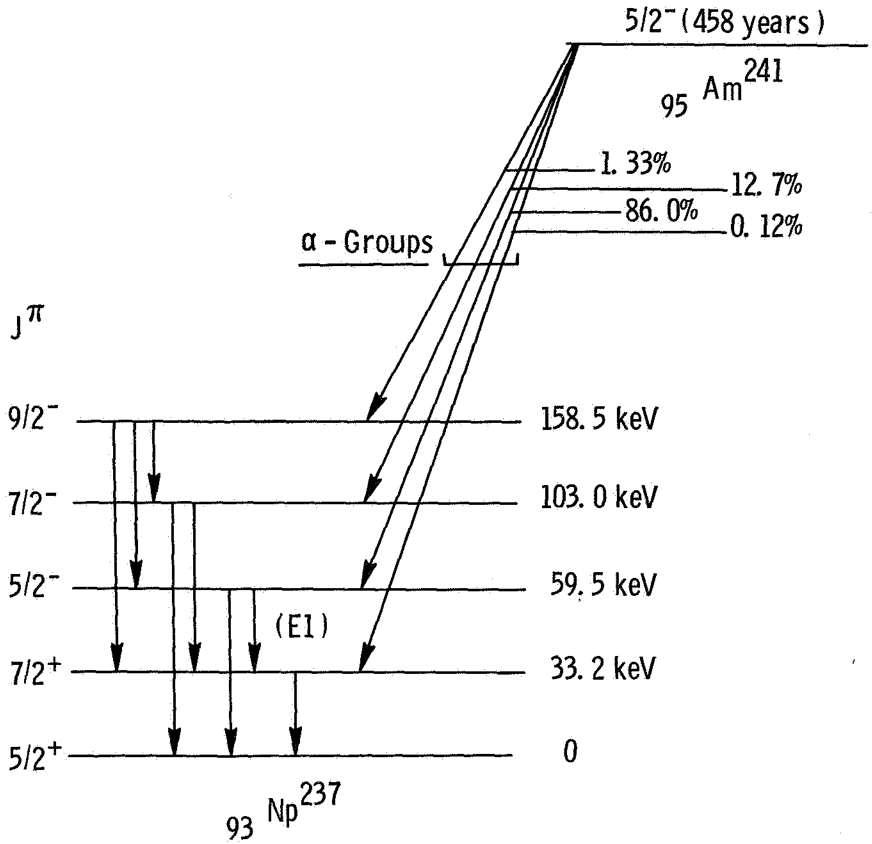

Figure 1. Decay scheme for $Am^{241} \xrightarrow{\alpha} Np^{237}$.

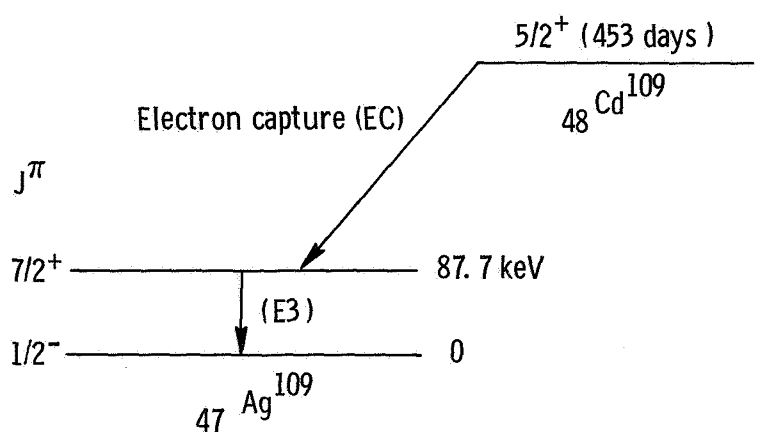

Figure 2. Decay scheme for $Cd^{109} \xrightarrow{EC} Ag^{109}$.

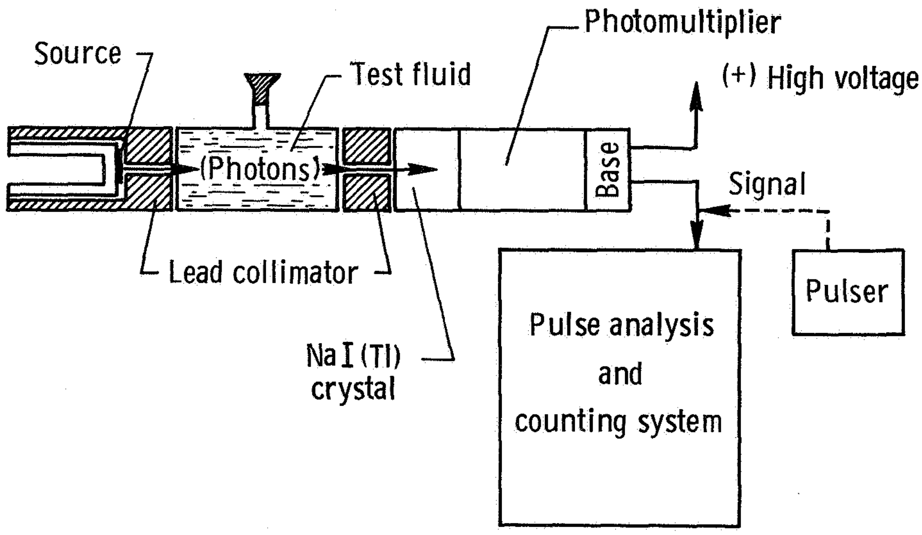

Figure 3. Schematic diagram of experimental system used for measuring attenuation coefficients of Am^{241} and Cd^{109} gamma rays.

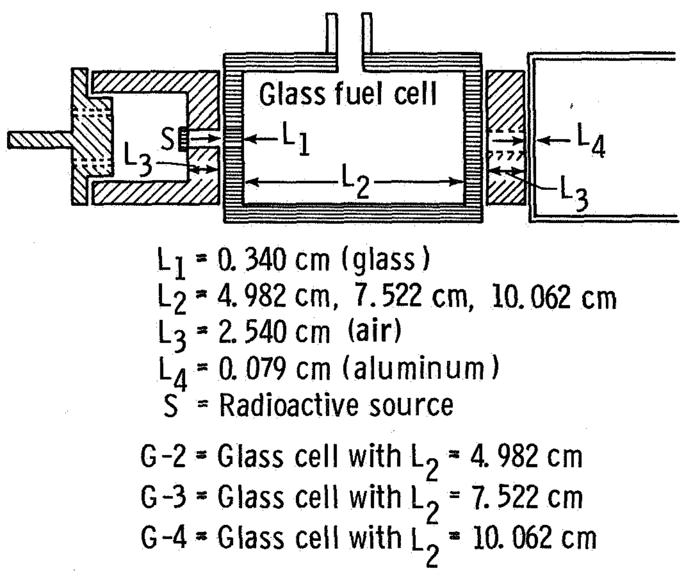

Figure 4. Geometrical details of fuel cell and associated shields/collimators.

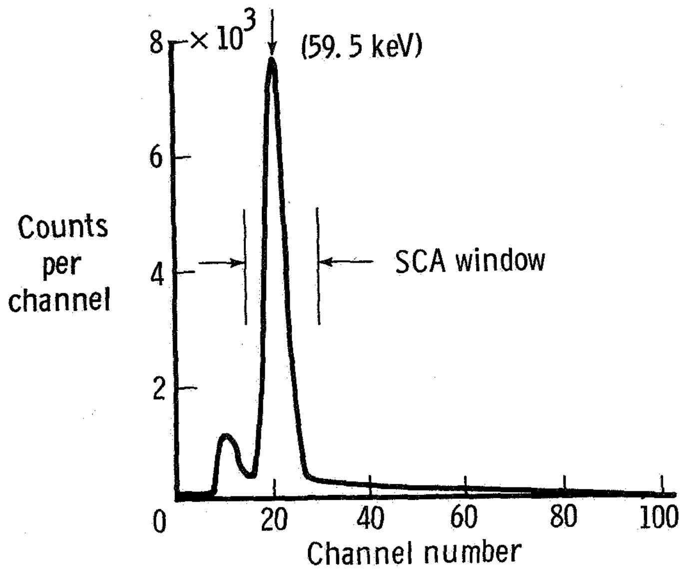

(a) Empty cell.

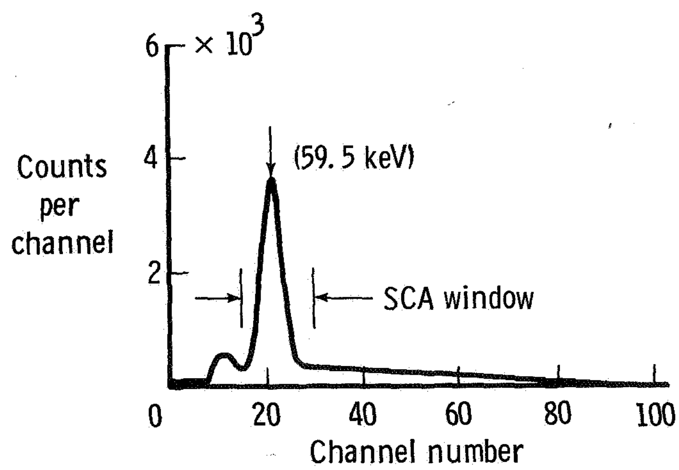

(b) Cell filled with Jet A fuel.

Figure 5. Typical spectra of Am^{241} (59.5 keV) radiation source through measurement cell.

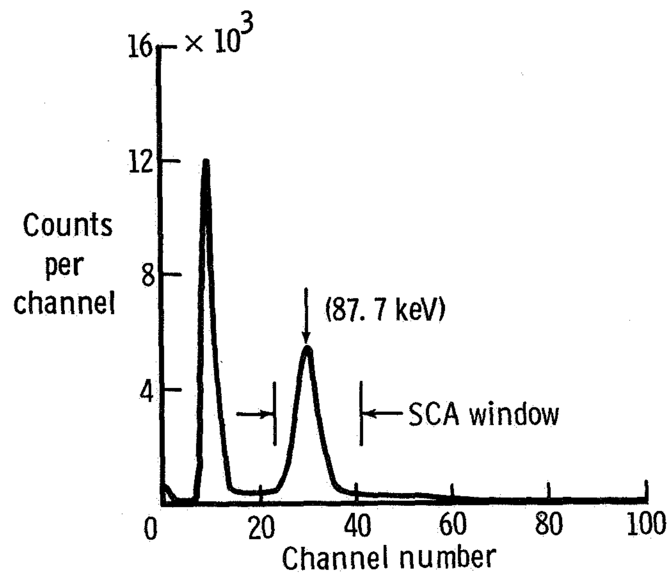

(a) Empty cell.

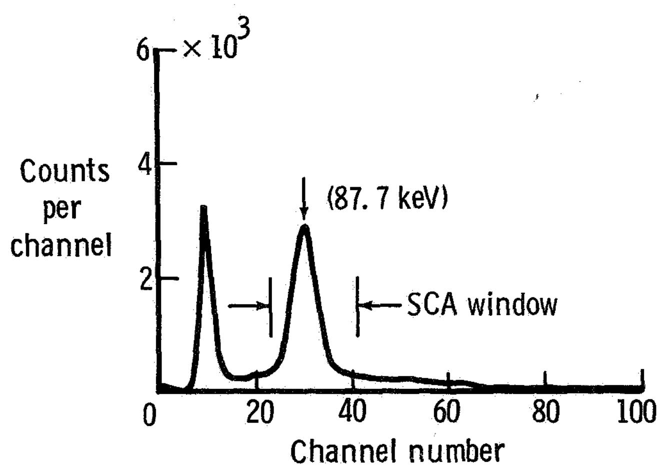

(b) Cell filled with Jet A fuel.

Figure 6. Typical spectra of Cd^{109} (87.7 keV) radiation source through measurement cell.

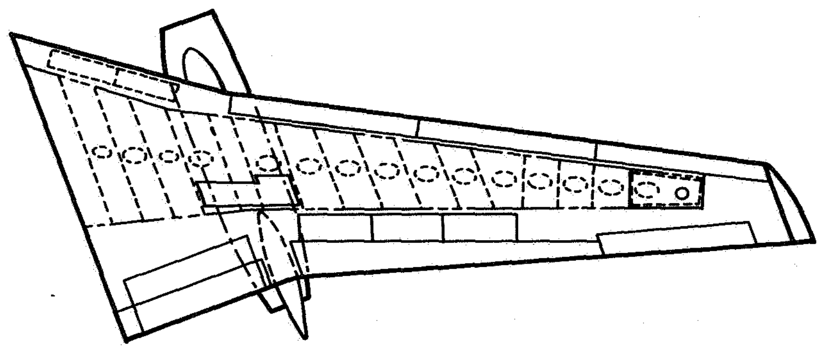

Figure 7. Wing compartment diagram for Boeing 737 airplane.

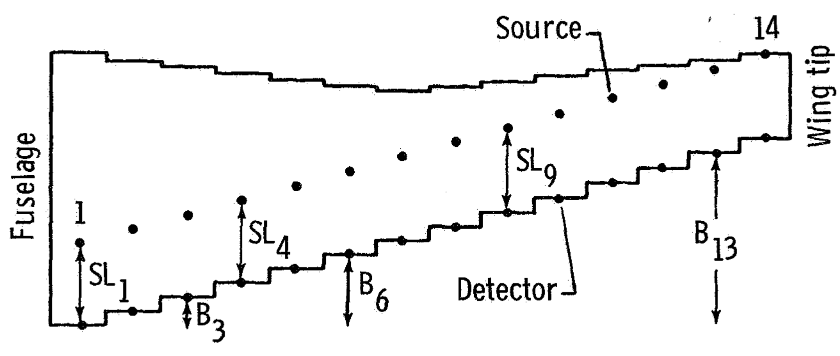

Figure 8. Vertical cross section of wing tank in flight.

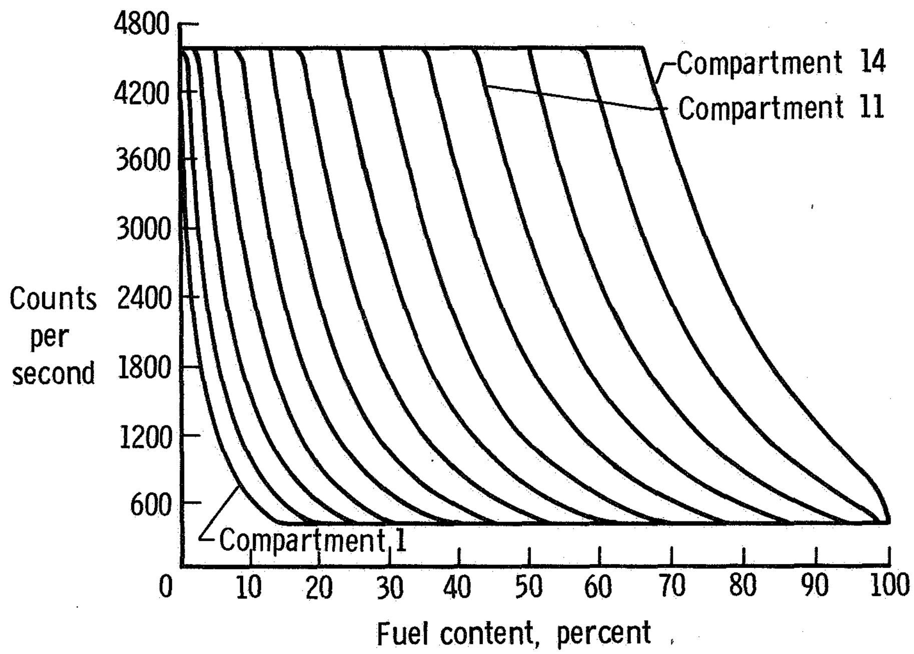

Figure 9. Counting rate versus fuel content in wing tank at various source-detector stations.

Standard Bibliographic Page

1. Report No.	2. Government Accession No.	3. Recipient's Catalog No.
NASA TM-87706		

4. Title and Subtitle
Feasibility of a Nuclear Gauge for Fuel Quantity Measurement Aboard Aircraft

5. Report Date
August 1986

6. Performing Organization Code
141-30-30-01

7. Author(s)
Jag J. Singh, Gerald H. Mall, Danny R. Sprinkle, and Hoshang Chegini

8. Performing Organization Report No.
L-16132

9. Performing Organization Name and Address
NASA Langley Research Center
Hampton, VA 23665-5225

ND210491

10. Work Unit No.

11. Contract or Grant No.

12. Sponsoring Agency Name and Address
National Aeronautics and Space Administration
Washington, DC 20546-0001

13. Type of Report and Period Covered
Technical Memorandum

14. Sponsoring Agency Code

15. Supplementary Notes
Jag J. Singh and Danny R. Sprinkle: Langley Research Center, Hampton, Virginia.
Gerald H. Mall: Computer Sciences Corporation, Hampton, Virginia. CZ788405
Hoshang Chegini: Old Dominion University, Norfolk, Virginia. DS853217

16. Abstract
Capacitance fuel gauges have served as the basis for fuel quantity indicating systems in aircraft for several decades. However, there have been persistent reports by the airlines that these gauges often give faulty indications due to microbial growth and other contaminants in the fuel tanks. This report describes the results of a feasibility study of using gamma ray attenuation as the basis for measuring fuel quantity in the tanks. Studies with a weak Am^{241} 59.5-keV radiation source indicate that it is possible to continuously monitor the fuel quantity in the tanks to an accuracy of better than 1 percent. These measurements also indicate that there are easily measurable differences in the physical properties and resultant attenuation characteristics of JP-4, JP-5, and Jet A fuels. The experimental results, along with a suggested source-detector geometrical configuration, are described.

17. Key Words (Suggested by Authors(s))
Nuclear gauge for aircraft fuel
Am^{241} source, linear attenuation
Coefficient, mass attenuation
Coefficient, self-calibrating system
Self-diagnosing system

18. Distribution Statement
Unclassified—Unlimited

Subject Category 35

19. Security Classif.(of this report)	20. Security Classif.(of this page)	21. No. of Pages	22. Price
Unclassified	Unclassified	23	A02

For sale by the National Technical Information Service, Springfield, Virginia 22161

NASA-Langley, 1986